TÜBİTAK

Turkish Journal of Medical Sciences

http://journals.tubitak.gov.tr/medical/

Research Article

Turk J Med Sci
(2022) 52: 762-769
© TÜBİTAK
doi:10.55730/1300-0144.5371

# Radiomics analysis of uterine tumors in 18F-fluorodeoxyglucose positron emission tomography for prediction of lymph node metastases in endometrial carcinoma

**Çiğdem SOYDAL[1,*], Bulut VARLI[2], Mine ARAZ[1], Batuhan BAKIRARAR[3], Salih TAŞKIN[2], Uğur Fırat ORTAÇ[2]**

[1]Department of Nuclear Medicine, Faculty of Medicine, Ankara University, Ankara, Turkey
[2]Department of Gynecological Oncology, Faculty of Medicine, Ankara University, Ankara, Turkey
[3]Department of Biostatistics, Faculty of Medicine, Ankara University, Ankara, Turkey

**Received:** 29.01.2021 • **Accepted/Published Online:** 27.02.2022 • **Final Version:** 16.06.2022

**Background/aim:** In this single-center study, we aimed to analyze texture features of primary uterine lesions on 18F-FDG PET/CT to predict lymph node metastases.

**Material and methods:** Totally, 157 (mean age: 62 ± 10.2 years) patients were included in the analysis. Histopathological examination results were considered as the standard reference for nodal involvement. On $^{18}$F-FDG PET/CT images, only the primary tumor was segmented. SUVmax, SUVmean, SUVpeak, MTV, and TLG of primary uterine lesions were calculated for analyses. For texture analysis first, second, and higher-order texture features were calculated.

**Results:** Mean diameter of primary uterine lesions was calculated as 35± 18.1 mm. Lymph node metastases were detected in 19% of patients in histopathological examination of surgical materials. While 26 patients had pelvic lymph node metastases, 19 patients had additional paraaortic lymph node metastases. On radiomics analysis for 20 features, a significant difference was found between patients with and without lymph node metastasis. With using data mining methods GLZLM ZLNU, $Entropy_{GLCM}$, $Entropy_{histo}$, GLRLM LRHGE, GLZLM HGZE, GLZLM SZHGE, GLRLM HGRE, GLRLM SRHGE were found significant radiomics features to predict lymph node metastasis with a diagnostic accuracy of 0.8.

**Conclusion:** The radiomics analysis of intratumoral heterogeneity is a promising method for improving triage of the patients for lymph node dissection in endometrial carcinoma.

**Key words:** Endometrial carcinoma, lymph node metastasis, $^{18}$F-FDG PET/CT, radiomics

## 1. Introduction

Endometrial carcinoma is the most common gynecological cancer worldwide [1]. Lymph nodes are the most common extrauterine spread site with the rate of 20% and the presence of lymph node metastasis is a prognostic factor for endometrial carcinoma patients [2,3]. Although surgery including bilateral pelvic and paraaortic lymphadenectomy is gold standard for nodal staging, the surgical management of the nodal disease is still controversial [4,5]. Randomized trials showed that pelvic lymphadenectomy had no impact on survival in early-stage endometrial carcinoma patients [6,7]. Considering the low rate of lymph node metastases, determination of lymph node status preoperatively would be beneficial for patient management to avoid surgery-related complications. In the last decade, sentinel lymph node (SLN) mapping has become a feasible option with high diagnostic accuracy in the management of clinically early-stage endometrial cancer [8]. However, the SLN algorithm suggests resection of only the mapped nodes without systematic lymphadenectomy even if the metastasis exists in the SLNs. Moreover, the status of SLNs for metastasis will be reported in the postoperative period and patients with SLN metastasis may have a need of a second surgery for systematic lymphadenectomy. Another limitation of SLN mapping is that it primarily focuses on pelvic lymph nodes and evaluation of the paraaortic area is not a standard. Thus, with this approach, isolated paraaortic metastases can be under-diagnosed [9,10].

With its high positive predictive value, $^{18}$F-FDG PET/CT is suggested as the best technique for endometrial carcinoma nodal staging, particularly in high-risk patients [11]. However, due to its low spatial resolution, metastatic lymph nodes smaller than 5 mm result in false-negative results [12]. Parameters reflecting the amount of $^{18}$F-FDG uptake in the lymph node or in primary uterine lesion have been studied. These were standardized uptake value

* Correspondence: csoydal@yahoo.com

(SUV) based parameters such as SUVmax, SUVpeak, SUVmean as well as metabolic tumor volume (MTV) and total lesion glycolysis (TLG) [12]. However, tumor $^{18}$F-FDG uptake shows the uneven spatial distribution, at least partly due to underlying biological tumor conditions such as metabolism, hypoxia, necrosis, and cellular proliferation, which is called intratumoral heterogeneity [12]. One of the most highlighted methods to quantify intratumoral heterogeneity from images is texture analysis. Because intratumoral heterogeneity is related to tumor aggressiveness, treatment response, and prognosis, the relationship between texture features of primary tumor focus, and lymph node metastases has been a subject of interest. Recently, a few studies have focused on the value of radiomics features of primary uterine tumors on PET images to improve sensitivity in the detection of lymph node metastases in patients with endometrial carcinoma [13,14]. In this single-center study, we aimed to analyze texture features of primary uterine lesions on 18F-FDG PET/CT to predict lymph node metastases.

## 2. Material and methods

### 2.1. Patient population

In this study, $^{18}$F-FDG PET/CT images of 191 patients who underwent surgical treatment for endometrial carcinoma were evaluated retrospectively. The study was approved by the local ethical committee (approval number: İ1-40-21). Nineteen patients were excluded because their primary tumors were non $^{18}$F-FDG avid. Additional 15 patients, with a tumor smaller than 64 voxels were excluded from the analysis. Finally, images of 157 patients were included in the analysis. All the included patients had undergone total hysterectomy, bilateral salpingo-oophorectomy, and at least bilateral pelvic lymphadenectomy. Histopathological examination results were considered as the standard reference for nodal involvement.

### 2.2. $^{18}$F-FDG PET/CT protocol and tumor segmentation

All the patients underwent $^{18}$FDG PET/CT for evaluation of the disease stage. Informed consent was obtained from all patients before imaging. PET/CT images were acquired with two PET/CT scanners, a GE Discovery ST and Discovery 710 (GE Medical Systems, Milwaukee, USA). Patients fasted at least 6 h before imaging and blood glucose levels were checked. Those with a blood glucose level above 150 mg/dL did not undergo scanning. Oral contrast was given to all patients. Images from the vertex to the proximal femur were obtained in the supine position. Whole-body $^{18}$F-FDG PET/CT imaging was performed approximately 1 h after intravenous injection of 296-370 MBq $^{18}$F-FDG. During the waiting period, patients rested in a quiet room without taking any muscle relaxants. PET images were acquired for 4 min per bed position. Emission PET images were reconstructed with noncontrast CT images. CT images were also obtained with a standardized protocol of 140 kV, 70 mA, tube rotation time of 0.5 s per rotation, a pitch of 6, and a slice thickness of 5 mm. Patients were allowed to breathe normally during the procedure. Attenuation-corrected PET/CT fusion images were reviewed in three planes (transaxial, coronal, and sagittal) on an AW VolumeShare 7 (GE Medical Systems, Milwaukee, USA) workstation. A board-certified nuclear medicine physician with more than 10 years' experience in PET/CT, segmented primary uterine lesions. $^{18}$F-FDG PET/CT images were evaluated with a semiautomatic approach. The volume of interest (VOI) of the uterine lesion was defined on PET images with a threshold of 40% of the maximum standardized uptake value (SUVmax) using commercial software (PET VCAR; GE Healthcare). Only the primary tumor was segmented. SUVmax, SUVmean, SUVpeak, MTV, and TLG of primary uterine lesions were calculated for analyses.

### 2.3. Texture feature extraction

Texture features (i.e. first-, second-, and higher-order imaging parameters) were extracted using dedicated software for radiomics (LIFEx) (https://www.lifexsoft.org/ index.php). For technical reasons, second and higher-order imaging parameters were extracted only for lesions greater than 64 voxels. Details of calculated first, second, and higher-order texture features are given in Table 1. An example of tumor delineation for texture analysis is given in Figure 1.

### 2.4. Statistical analysis

WEKA 3.7 and SPSS 11.5 programs were used to evaluate the data. Descriptives were presented as mean ± standard deviation and median (minimum-maximum) for quantitative variables and number of patients (percent) for qualitative variables. In order to investigate whether there is a statistically significant difference between the qualitative variables with lymph node metastasis positive and negative groups. Mann-Whitney U test was used since the normal distribution assumptions were not met. The statistical significance level was taken as 0.05. Classification methods of Support Vector Machine, Hoeffding Tree, J48, and Multilayer Perceptron were used in the WEKA program. The data set was evaluated using the 10-fold cross-validation test option. Accuracy, F-Measure, Precision, Recall, and Precision-Recall Curve (PRC Area) were used as data mining performance criteria of textural features of primary uterine tumors to predict lymph node metastasis.

## 3. Results

### 3.1. Patients

Images of 157 (mean age: 62 ± 10.2 years) women who underwent an $^{18}$F-FDG PET/CT scan with the diagnosis

**Table 1.** List of the studied radiomics features.

| **The first-order** | **The higher-order** |
|---|---|
| SUVmax | GLRLM SRE |
| SUVmean | GLRLM LRE |
| SUVpeak | GLRLM LGRE |
| MTV | GLRLM HGRE |
| TLG | GLRLM SRLGE |
| Skewness | GLRLM SRHGE |
| Kurtosis | GLRLM LRLGE |
| $Entropy_{histo}$ | GLRLM LRHGE |
| Energy | GLRLM GLNU |
| SHAPE Sphericity | GLRLM RLNU |
| SHAPE Compacity | GLRLM RP |
| | GLZLM SZE |
| **The second-order** | GLZLM LZE |
| $Homogenity_{GLCM}$ | GLZLM LGZE |
| $Energy_{GLCM}$ | GLZLM HGZE |
| $Contrast_{GLCM}$ | GLZLM SZLGE |
| $Correlation_{GLCM}$ | GLZLM SZHGE |
| $Entropy_{GLCM}$ | GLZLM LZLGE |
| $Dissimilarity_{GLCM}$ | GLZLM LZHGE |
| | GLZLM GLNU |
| | GLZLM ZLNU |
| | GLZLM ZP |
| | $Coarseness_{NGLDM}$ |
| | $Contrast_{NGLDM}$ |
| | $Busyness_{NGLDM}$ |

*SUV* standardized uptake value, *MTV* metabolic tumor volume, *TLG* total lesion glycolysis, *GLCM* gray-level cooccurence matrix, *GLRLM* gray-level run-length matrix, *SRE* short-run emphasis, *LRE* long-run emphasis, *LGRE* low gray-level run emphasis, *HGRE* high gray-level run emphasis, *SRLGE* short-run low gray-level emphasis, *SRHGE* short-run high gray-level emphasis, *LRLGE* long-run low gray-level emphasis, *LRHGE* long-run high gray-level emphasis, *GLNU* gray-level nonuniformity, *RP* run percentage, *GLZLM* gray level zone length matrix, *SZE* short-zone emphasis, *LZE* long-zone emphasis, *LGZE* low gray-level zone emphasis, *HGZE* high gray-level zone emphasis, *SZLGE* short-zone low gray-level emphasis, *SZHGE* short-zone high gray-level emphasis, *LZLGE* long-zone low gray-level emphasis, *LZHGE* long-zone high gray-level emphasis, *ZLNU* zone length nonuniformity, *ZP* zone percentage, *NGLDM* neighborhood grey-level different matrix.

of endometrial carcinoma between March 2012 and July 2019 were analyzed. Details of the study population are presented in Table 2. The mean diameter of primary uterine lesions was calculated as 35 ± 18.1 mm. Lymph node metastases were detected in 30 (19%) of patients in histopathological examination of surgical materials. While 26 patients had pelvic lymph node metastases, 19 patients had paraaortic lymph node metastases.

### 3.2. Texture analysis of $^{18}$F-FDG PET images and data mining

Descriptive data of texture parameters for lymph node metastasis positive and negative patient groups are provided in Table 3. On radiomics analysis for 20 features, a significant difference was found between patients with and without lymph node metastasis.

Information Gain Attribute Eval and Gain Ratio Attribute Eval methods in WEKA were used because there were too many variables in the data set. With using these methods, the importance of the variables and the values it added to the data set were examined. The variables, which were determined to be insignificant by two methods and considered to be unimportant as clinical information, were excluded from the data set. A total of 9 variables (8 independent variables and 1 dependent variable) remained finally. These variables were GLZLM ZLNU, $Entropy_{GLCM}$, $Entropy_{histo}$, GLRLM LRHGE, GLZLM HGZE, GLZLM SZHGE, GLRLM HGRE, GLRLM, SRHGE, and lymph node metastases. Percentages of variable importance according to dependent variable lymph node metastases are given in Figure 2.

Looking at the data mining results in Table 4, the Support Vector Machine, Hoeffding Tree, and J48 gave similar results according to Accuracy and F-measure criteria, which are the most accepted performance criteria. Multilayer perceptron was found to be the worst serving method. The diagnostic accuracy of texture parameters was calculated at about 0.8 for the prediction of lymph node metastasis.

## 4. Discussion

Due to the limited spatial resolution of $^{18}$F-FDG PET, metastatic lymph nodes smaller than 5 mm cannot be diagnosed accurately and this can cause false-negative findings [11]. In this study, we aimed to investigate the efficacy of radiomics analysis of the primary uterine lesion to improve the sensitivity of $^{18}$F-FDG PET in detecting nodal metastases. We analyzed standard imaging features like SUV, MTV, and TLG, together with the first, second, and higher-order texture features.

The concept of radiomics is defined as the high-throughput extraction of a large number of features from medical images [15,16]. It is assumed that genomic and proteomic cancer patterns are expressed in image-based features and with optimal analysis of medical images such as texture analysis, cancer properties can be quantified [12,16]. Texture analysis has long been applied in CT

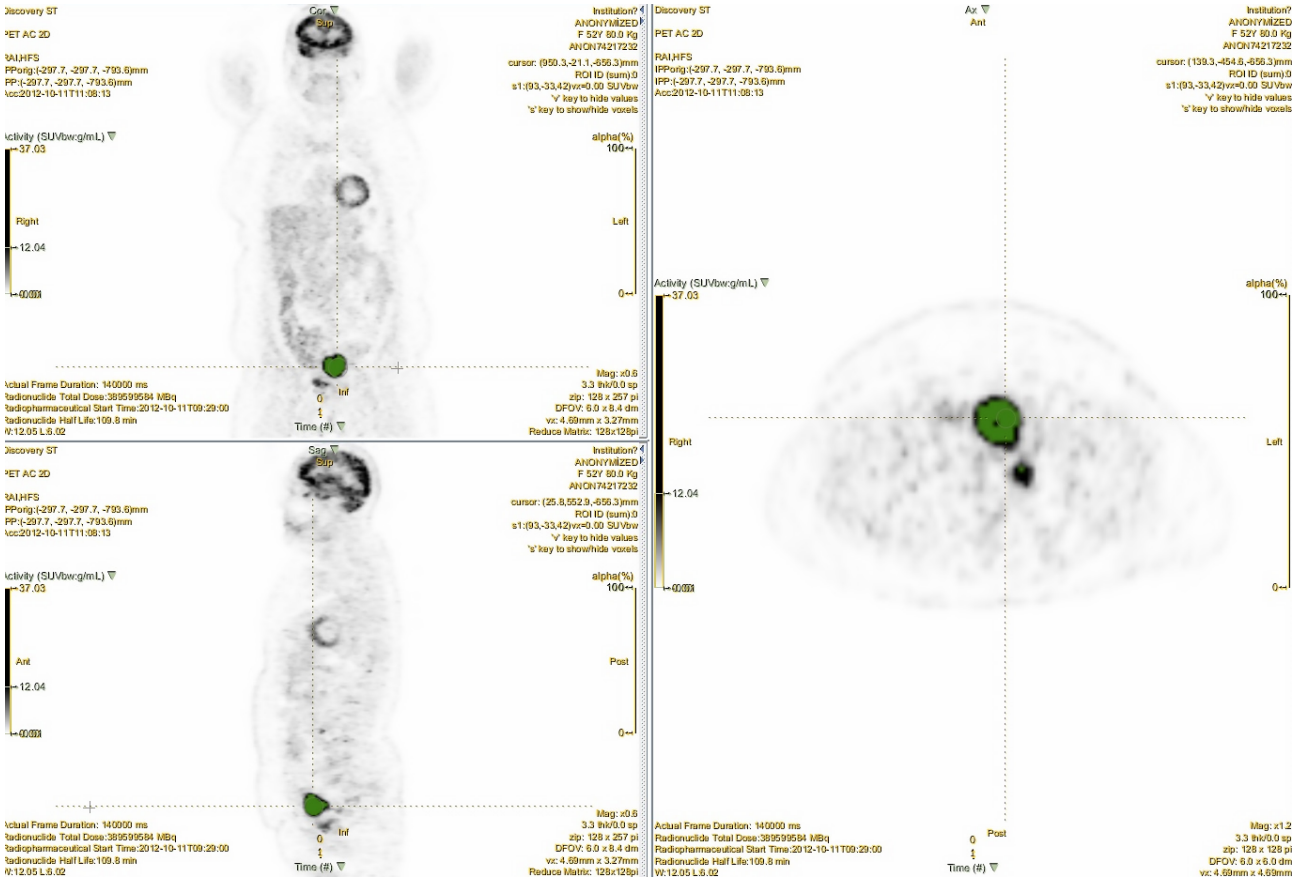

**Figure 1.** An example for tumor delineation for texture analysis.

and magnetic resonance imaging (MRI), but it has been adapted to PET imaging very recently [14]. As the most widely used PET feature; SUVmax of primary uterine lesions, is considered as an important indicator reflecting tumor aggressiveness, such as myometrial invasion or tumor grade. However, it was not significantly correlated with lymph node status according to previous studies [17,18]. Contrarily to SUVmax other semiquantitative parameters, MTV and TLG seem to have a predictive role for lymph node status. Endometrial tumors with higher MTV and TLG have a higher tendency to spread to lymph nodes than without [19].

In our analyses, descriptive parameters of SUVpeak, MTV, and TLG of patients with and without lymph node metastasis were found significantly different. However, they did not remain significant in the data mining methods. In the data mining methods, one first, one second, and six higher-order texture parameters were found significant to predict lymph node metastases. GLZLM ZLNU showed the best performance for nodal staging in data mining. It is a higher-order texture feature and is described as the length of the homogeneous zones in the gray level zone length matrix. It has been reported as the best texture parameter for discrimination of squamous cell carcinoma and adenocarcinoma of the lung [20]. Similarly, patients with estrogen negative breast tumors were reported higher GLZLM ZLNU than positive ones [21]. Moreover, Wang et al. published prognostic value of functional parameters of $^{18}$F-FDG PET/CT in patients with renal/adrenal lymphoma. They have reported that the tumor stage, Entropy $_{GLCM}$, GLZLM GLNU, and GLZLM ZLNU values were significant predictors of overall survival [22]. Entropy $_{GLCM}$ which is described as the randomness of grey-level voxel pairs was the second most significant texture feature in our series.

When we take a look at the PET radiomics studies in endometrial carcinoma patients, data is limited in the literature [13,14]. Bernardi et al. reported their data for texture analysis of $^{18}$F-FDG PET images of endometrial carcinoma patients. They found that the zone percentage of the grey level size zone matrix, (GLSZM ZP) was able to predict LN metastases better than any other feature. Also, they reported that the combination of visual detection and GLSZM ZP values increased the sensitivity of lymph node metastasis detection [13]. In another study, Crivellaro et al. reported the results of the combination of PET/CT,

**Table 2.** Characteristics of the patient population.

| **Parameter** | |
|---|---|
| *Age (mean ± SD, years)* | 62.0 ± 10.2 |
| *Menopausal state (n,%)* | |
| Premenopausal | 25 (15.9%) |
| Postmenopausal | 132 (84.1%) |
| *Grade (n,%)* | |
| G1 | 44 (28.0%) |
| G2 | 56 (35.6%) |
| G3 | 57 (36.4%) |
| *Histology (n, %)* | |
| Endometrioid | 124 (79.0%) |
| Clear cell/serous/mucinous/mixed | 21 (13.4%) |
| Malignant mesodermal tumor | 12 (7.6%) |
| *Myometrial invasion (n %)* | |
| None | 11 (7.0%) |
| <50% | 74 (47.1%) |
| >50% | 72 (45.9%) |
| *FIGO Stage (n, %)* | |
| I | 112 (71.3%) |
| II | 12 (7.6%) |
| III | 26 (16.6%) |
| IV | 7 (4.5%) |
| *Lymph node metastases (n,%)* | |
| Yes | 30 (19.1%) |
| No | 127 (80.9%) |

*FIGO:* Federation of Gynecology and Obstetrics

radiomics, and sentinel lymph node mapping for nodal staging of endometrial cancer patients. They found a significant association between the presence of lymph node metastases and 64 features on radiomics analysis. Volume-density was the most predictive feature. They concluded that PET radiomics features of the primary tumor seemed promising for the prediction of nodal metastases, which were not detected by visual analysis [14]. In endometrial carcinoma patients, different radiomics features have been reported as the best predictor for lymph node metastases. That might be related to the limited number of included patients and the different distribution of risk groups between studies. In our study, differently from previous ones, we used cross-validation method for data mining. Cross-validation is the recommended method for analyzing all data with more precise metrics [23]. Although different texture features showed significant distribution among patients with and without lymphatic metastases, results of our analysis and previously reported ones support the idea that radiomics analysis of PET images of primary uterine lesions is a promising method to define lymph node metastasis. Standardized, randomized studies with large patient populations would help validation of texture features to predict lymph node metastasis of endometrial carcinoma.

In routine clinical practice, lymphadenectomy decision is given according to risk factors-grade, myometrial invasion and tumor type- provided by preoperative endometrial biopsy or intraoperative frozen section examination. However, unnecessary lymphadenectomy is still possible for many patients despite the use of these methods. Instead of this approach, the SLN algorithm seems to be a more convenient method, but low volume metastases are also diagnosed by the SLN ultrastaging procedure, and the sensitivity of $^{18}$F-FDG PET CT in the diagnosis of lymphatic metastases decreases. With the combined use of radiomics and SLN mapping [14], patients who are candidates for SLN mapping and ultrastaging can be determined, even for low-volume disease, and patients at risk for lymphatic metastasis can be more accurately identified. We planned to investigate the diagnostic accuracy of a combination of SLN mapping and radiomics in another study.

This study is one of the very few studies evaluating radiomics in endometrial cancer, and our results may guide future studies. However, the retrospective design and the small number of patients were the major limitations of our study. Although we have not correlated oncologic outcomes with radiomics analysis, future studies may show a correlation of these two features and this knowledge could help clinicians in planning patient-based treatment and follow-up protocols. In this study, we analyzed data of two different PET/CT scanners. It should be kept in mind that accurate results cannot be achieved in the data of two different PET/CT scanners, even if they were performed using the same protocol. Since this may cause heterogeneity in the images and the results obtained. Another limitation of the study is that the radiomics analysis results in combination with SLN mapping are missing. Lastly, dealing with high data input made results technically complex. As the studies come across, several models would be created, and this complex situation could then be overcome.

## 5. Conclusion

The radiomics analysis of intratumoral heterogeneity is a promising method for improving triage of the patients for lymph node dissection in endometrial carcinoma. However, multicenter studies with larger patient populations are needed for validation.

**Table 3.** Descriptives for lymph node metastases.

| Variables | Lymph node metastasis | | | | |
|---|---|---|---|---|---|
| | No (n = 127) | | Yes (n = 30) | | |
| | Mean ± SD | Median (min-max) | Mean ± SD | Median (min-max) | p value |
| SUVpeak | 8.88 ± 7.81 | 9th June (0.00–30.28) | 12.83 ± 7.35 | 15.13 (0.00–27.67) | 0.008 |
| TLG | 115.81 ± 180.55 | 45.55 (5.13–1227.41) | 300.17 ± 418.73 | 156.97 (9.21–2209.97) | <0.001 |
| $Entropy_{histo}$ | 1.19 ± 0.21 | January 22 (0.00–1.58) | 1.28 ± 0.25 | January 36 (0.60–1.57) | 0.002 |
| Energy | 0.09 ± 0.10 | 0.07 (0.03–1.00) | 0.09 ± 0.09 | 0.05 (0.03–0.47) | 0.007 |
| MTV | 11.55 ± 13.83 | June 18 (0.52–85.00) | 25.11 ± 29.59 | 14.29 (2.01–150.60) | <0.001 |
| $Energy_{GLCM}$ | 0.02 ± 0.03 | 0.01 (0.00–0.34) | 0.02 ± 0.06 | 0.01 (0.00–0.34) | 0.037 |
| $Contrast_{GLCM}$ | 57.29 ± 52.40 | 47.50 (0.00–228.46) | 73.94 ± 43.28 | 66.39 (0.00–174.36) | 0.032 |
| $Correlation_{GLCM}$ | 0.17 ± 0.15 | 0.16 (–0.10–0.58) | 0.28 ± 0.18 | 0.24 (0.00–0.63) | 0.004 |
| $Entropy_{GLCM}$ | 1.61 ± 0.84 | January 84 (0.00–2.75) | 2.10 ± 0.69 | February 24 (0.00–2.82) | <0.001 |
| $Dissimilarity_{GLCM}$ | 4.98 ± 3.20 | May 43 (0.00–12.14) | 6.26 ± 2.52 | June 29 (0.00–10.72) | 0.036 |
| GLRLM HGRE | 849.27 ± 891.45 | 550.55 (0.00–3446.93) | 1325.28 ± 825.50 | 1337.62 (0.00–3584.94) | 0.001 |
| GLRLM SRHGE | 803.31 ± 814.99 | 536.24 (0.00–3044.55) | 1245.22 ± 707.57 | 1294.08 (0.00–2630.25) | 0.002 |
| GLRLM LRHGE | 1332.78 ± 3300.98 | 609.35 (0.00–34583.96) | 2118.29 ± 3716.78 | 1472.90 (0.00–21,168.33) | 0.001 |
| GLRLM GLNU | 15.45 ± 29.84 | August 25 (0.00–279.51) | 21.64 ± 21.04 | 14th June (0.00–84.61) | 0.014 |
| GLRLM RLNU | 174.91 ± 229.61 | 108.71 (0.00–1453.19) | 376.92 ± 390.69 | 242.75 (0.00–1778.01) | 0.001 |
| GLZLM HGZE | 822.53 ± 816.52 | 564.47 (0.00–3153.00) | 1294.76 ± 751.74 | 1339.45 (0.00–3164.98) | 0.001 |
| GLZLM SZHGE | 630.12 ± 660.65 | 382.74 (0.00–2444.10) | 984.46 ± 627.32 | 980.51 (0.00-2828.95) | 0.002 |
| GLZLM LZHGE | 102,276.19 ± 903,259.46 | 2686.92 (0.00–10,085,856.18) | 116,072.17 ± 578,882.13 | 6288.71 (0.00–3,179,985.77) | 0.005 |

**Table 3.** (Continued).

| | | | | | |
|---|---|---|---|---|---|
| GLZLM GLNU | 6.17 ± 6.96 | 4th July | 10.84 ± 9.47 | August 34 | 0.002 |
| | | (0.00–36.85) | | (0.00–43.27) | |
| GLZLM ZLNU | 54.79 ± 68.57 | 30.25 | 115.81 ± 111.29 | 95.10 | <0.001 |
| | | (0.00–361.54) | | (0.00–566.81) | |

*SUV* standardized uptake value, *MTV* metabolic tumor volume, *TLG* total lesion glycolysis, *GLCM* gray-level cooccurence matrix, *GLRLM* gray-level run-length matrix, *HGRE* high gray-level run emphasis, *SRHGE* short-run high gray-level emphasis, *LRHGE* long-run high gray-level emphasis, *GLNU* gray-level nonuniformity, *HGZE* high gray-level zone emphasis, *SZHGE* short-zone high gray-level emphasis, *LZHGE* long-zone high gray-level emphasis, *ZLNU* zone length nonuniformity.

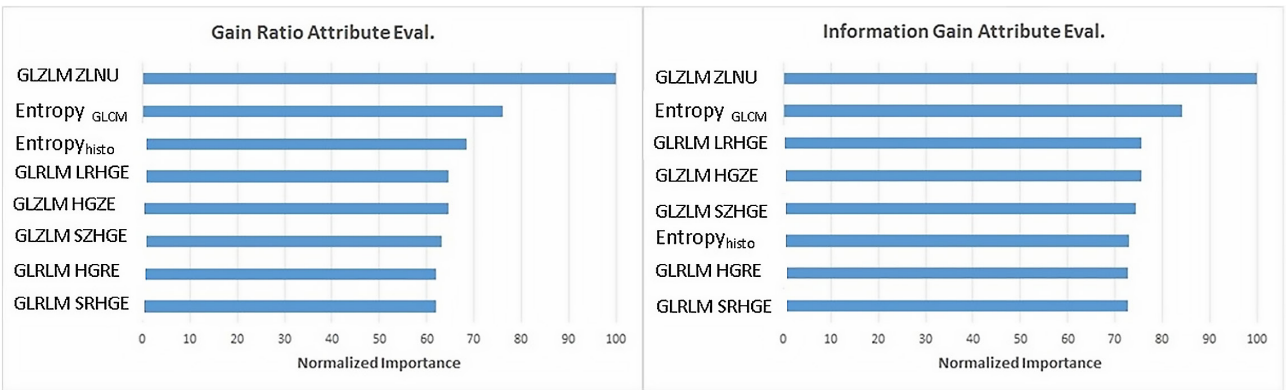


**Figure 2.** Variable importance for metastases.

**Table 4.** Performance comparison of data mining methods.

| Methods | F-Measure | Precision | Recall | PRC Area |
|---|---|---|---|---|
| **Support vector machine** | 0.723 | 0.655 | 0.808 | 0.691 |
| **Hoeffding Tree** | 0.723 | 0.655 | 0.808 | 0.688 |
| **J48** | 0.731 | 0.720 | 0.803 | 0.701 |
| **Multilayer perceptron** | 0.736 | 0.716 | 0.771 | 0.745 |

**Acknowledgment/Disclaimers/Conflict of interest**
Authors disclose there is no conflict of interest.

**Informed consent**
A local ethical committee approval was obtained for this study and all participants provided informed consent.

## References

1. Ferlay J, Soerjomataram I, Dikshit R, Eser S, Mathers C et al. Cancer incidence and mortality worldwide: sources, methods and major patterns in GLOBOCAN 2012. International Journal of Cancer 2015; 136 (5): E359-386. doi: 10.1002/ijc.29210
2. Jemal A, Murray T, Ward E, Samuels A, Tiwari RC et al. Cancer statistics. CA A Cancer Jornal of Clinicians 2005; 55 (1): 10-30. doi: 10.3322/canjclin.55.1.10
3. Lewin SN, Herzog TJ, Medel NIB, Deutsch I, Burke WM et al. Comparative performance of the 2009 international federation of gynecology and obstetrics' staging system for uterine corpus cancer. Obstetrics and Gynecology 2010; 116 (5): 1141-1149. doi: 10.1097/AOG.0b013e3181f39849
4. Mariani A, Dowdy SC, Cliby WA, Gostout BS, Jones MB et al. Prospective assessment of lymphatic dissemination in endometrial cancer: a paradigm shift in surgical staging. Gynecological Oncology 2008; 109: 11-18. doi: 10.1016/j.ygyno.2008.01.023

5. Dowdy SC, Borah BJ, Bakkum-Gamez JN, Weaver AL, McGree ME et al. Prospective assessment of survival, morbidity, and cost associated with lymphadenectomy in low-risk endometrial cancer. Gynecological Oncology 2012; 127: 5-10. doi: 10.1016/j.ygyno.2012.06.035

6. Seracchioli R, Solfrini S, Mabrouk M, Facchini C, Di Donato N et al. Controversies in surgical staging of endometrial cancer. Obstetrics and Gynecology International 2010; 2010: 181963. doi: 10.1155/2010/181963

7. Kitchener H, Swart AM, Qian Q, Amos C, Parmar MK. Efficacy of systematic pelvic lymphadenectomy in endometrial cancer (MRC ASTEC trial): a randomised study. Lancet 2009; 373 (9658): 125-136. doi 10.1016/S0140-6736(08)61766-3

8. Crivellaro C, Baratto L, Dolci C, De Ponti E, Magni S et al. Sentinel node biopsy in endometrial cancer: an update. Clinical Translational Imaging 2018; 6 (2): 91-100. doi: 10.1007/s40336-018-0268-9

9. Türkmen O, Başaran D, Karalök A, Cömert Kimyon G, Taşçı T et al. Prognostic effect of isolated paraaortic nodal spread in endometrial cancer. Journal of the Turkish-German Gynecological Association 2018; 19 (4): 201-205. doi: 10.4274/jtgga.2017.0152

10. Taskın S, Sarı ME, Altın D, Ersöz CC, Gökçe A et al. Risk factors for failure of sentinel lymph node mapping using indocyanine green/near-infrared fluorescent imaging in endometrial cancer. Archives of Gynecology and Obstetrics 2019; 299 (6): 1667-1672. doi: 10.1007/s00404-019-05137-5

11. Signorelli M, Crivellaro C, Buda A, Guerra L, Fruscio R et al. Staging of high-risk endometrial cancer with PET/CT and sentinel lymph node mapping. Clinical Nuclear Medicine 2015; 40 (10): 780-785. doi: 10.1097/RLU.0000000000000852

12. Lee JW, Lee SM. Radiomics in Oncological PET/CT: Clinical Applications. Nuclear Medicine and Molecular Imaging 2018; 52 (3): 170-189. doi: 10.1007/s13139-017-0500-y

13. De Bernardi E, Buda A, Guerra L, Vicini D, Elisei F et al. Radiomics of the primary tumour as a tool to improve 18F-FDG-PET sensitivity in detecting nodal metastases in endometrial cancer European Journal of Nuclear Medicine and Molecular Imaging Research. 2018; 8: 86. doi: 10.1186/s13550-018-0441-1

14. Crivellaro C, Landoni C, Elisei F, Buda A, Bonacina M et al. Combining positron emission tomography/computed tomography, radiomics, and sentinel lymph node mapping for nodal staging of endometrial cancer patients. International Journal of Gynecological Cancer 2020; 30 (3): 378-382. doi: 10.1136/ijgc-2019-000945

15. Hatt M, Tixier F, Visvikis D, Le Rest CC. Radiomics in PET/CT: more than meets the eye? Journal of Nuclear Medicine 2017; 58: 365-366. doi: 10.2967/jnumed.116.184655

16. Lambin P, Rios-Velazquez E, Leijenaar R, Carvalho S, van Stiphout RG et al. Radiomics: extracting more information from medical images using advanced feature analysis. European Journal of Cancer 2012; 48: 441-446. doi: 10.1016/j.ejca.2011.11.036

17. Nakamura K, Hongo A, Kodama J, Hiramatsu Y. The measurement of SUVmax of the primary tumor is predictive of prognosis for patients with endometrial cancer. Gynecological Oncology 2011; 123(1): 82-87. doi: 10.1016/j.ygyno.2011.06.026

18. Nakamura K, Kodama J, Okumura Y, Hongo A, Kanazawa S et al. The SUVmax of 18F-FDG PET correlates with histological grade in endometrial cancer. International Journal of Gynecological Cancer. 2010; 20 (1): 110-115. doi: 10.1111/IGC.0b013e3181c3a288

19. Crivellaro C, Signorelli M, Guerra L, De Ponti E, Pirovano C et al. Tailoring systematic lymphadenectomy in high-risk clinical early stage endometrial cancer: the role of 18F-FDG PET/CT. Gynecological Oncology 2013; 130 (2): 306–311. doi: 10.1016/j.ygyno.2013.05.011

20. Hyun SH, Ahn MS, Koh YW, Lee SJ. A Machine-Learning Approach Using PET-Based Radiomics to Predict the Histological Subtypes of Lung Cancer, Clinical Nuclear Medicine 2019; 44: 956-960. doi: 10.1097/RLU.0000000000002810

21. Acar E, Turgut B, Yigit S, Kaya GC. Comparison of the volumetric and radiomics findings of 18F-FDG PET/CT images with immunohistochemical prognostic factors in local/locally advanced breast cancer. Nuclear Medicine Communications 2019; 40: 764-772. doi: 10.1097/MNM.0000000000001019

22. Wang M, Xu H, Xiao L, Song W, Zhu S et al. Prognostic Value of Functional Parameters of 18 F-FDG-PET Images in Patients With Primary Renal/Adrenal Lymphoma, Contrast Media and Molecular Imaging 2019; 2641627. doi: 10.1155/2019/2641627

23. https://towardsdatascience.com/5-reasons-why-you-should-use-cross-validation-in-your-data-science-project-8163311a1e79.